Singh, A., F. Seitz, C. Schwatke: Inter-annual water storage changes in the Aral Sea from multi-mission satellite altimetry, optical remote sensing, and GRACE satellite gravimetry. Remote Sensing of Environment, 123, 187-195, 2012.

DOI: 10.1016/j.rse.2012.01.001

Inter-annual Water Storage Changes in the Aral Sea from Multi-mission Satellite Altimetry, Optical Remote Sensing, and GRACE Satellite Gravimetry

Alka Singh (1), Florian Seitz (1) and Christian Schwatke (2)

(1) Earth Oriented Space Science and Technology (ESPACE), Technische Universität München, Arcisstr. 21, 80333 Munich, Germany, alka.singh@bv.tum.de

(2) Deutsches Geodätisches Forschungsinstitut, Alfons-Goppel-Str.11, 80539 Munich, Germany.

Abstract

The estimation of water storage variations in lakes is essential for water resource management activities in a region. In areas of ungauged or poorly gauged water bodies, satellite altimetry acts as a powerful tool to measure changes in surface water level. Remote sensing provides images of temporal coastline variations, and a combination of both measurement techniques can indicate a change in water volume. In this study variations of the water level of the Aral Sea were computed for the period 2002-2011 from the combination of radar and laser satellite altimetry data sets over the lake. The estimated water levels were analyzed in combination with coastline changes from Landsat images in order to obtain a comprehensive picture of the lake water changes. In addition to these geometrical observations temporal changes of water storage in the lake and its surrounding were computed from GRACE satellite gravimetry. With respect to its temporal evolution the GRACE results agree very well with the geometrical changes determined from altimetry and Landsat. The advancing desiccation until the beginning of 2009 and a subsequent abrupt gain of water in 2009-2010 due to exceptional discharge from Amu Darya can clearly be identified in all data sets.

Key words: Aral Sea, satellite altimetry, optical remote sensing, satellite gravimetry, GRACE, water mass variation.

Running Title: Water Storage Changes in the Aral Sea.

1. Introduction

Water stored in surface reservoirs (i.e. lakes and rivers) is the best accessible form for human consumption. But at the same time terrestrial surface water is one of the most uncertain components of continental hydrology with respect to its spatial and temporal distribution (Solomon et al., 2007). In this study we address the Aral Sea, a saline lake located in an arid zone of central Asia at 45° north and 60° east. Until 1960, it was the fourth largest lake worldwide after the Caspian Sea, Lake Superior and Lake Victoria (Zavialov, 2005). From then onwards it experienced a devastating decline, mainly due to diversion of water from its two primary inlet rivers the Amu Darya and the Syr Darya for agricultural purposes (Micklin, 1988; Bortnik, 1999; Crétaux et al., 2005).

Temporal variations of the level and the surface extent of the water body are linked to the changes in water storage and can be traced in observations of satellite altimetry and in optical or radar remote sensing images. Unfortunately for several years, availability of continuous in-situ water level observations has been limited in this region. A few gauge stations are located upstream, but due to evaporation and infiltration from canals, which were built on sand without sufficient sealing, an unknown fraction of water runoff may be lost in-between the observation point and the lake (Froebrich & Kayumov, 2004). Satellite altimetry was designed to measure oceanic surface water height but has demonstrated its potential for estimating changes in the level of terrestrial water bodies as well (Morris & Grill, 1994; Birkett, 1995; Cazenave et al., 1997; Prigent et al., 2007; Getirana et al., 2009) and has already been used on the Aral Sea (Crétaux et al., 2005; Crétaux et al., 2008; Kouraev et al., 2008; Calmant et al., 2009). MODIS Terra images (250 meter spatial resolution) were used by Kravtsova (2005) to observe seasonal variations in the Aral Sea surface in spring and autumn for the period 2000-2004. Since the spatial extent of the affected region is large related changes of water mass can be

identified in observations of temporal variations of the Earth's gravity field from space. The dedicated satellite mission GRACE has been continuously monitoring gravity field variations since almost a decade at a spatial resolution of about 300 km and a temporal resolution of better than one month. GRACE satellite gravity data was used in many studies to estimate terrestrial water storage changes (Ramillien et al., 2005; Güntner, 2008; Seitz et al., 2008; Werth et al., 2009). Large parts of the gravity signal (tides, atmosphere, and oceans) are already removed during pre-processing; consequently the remaining signals mainly reflect changes in water storage in the region.

In our study we compare the results of geometrical and gravimetrical space and in-situ observation techniques for the time frame between 2002 and 2011. The usefulness of the combination of heterogeneous data sets has previously been demonstrated for other surface water bodies, e.g. for the East African lakes (Becker et al., 2010), the Amazon (Frappart et al, 2008) or the Ganges (Papa et al., 2008). In Section 2 variations of the water level in the Aral Sea and its sub basins from satellite altimetry will be presented and discussed. Section 3 outlines the geometrical variations of the lake surface from optical remote sensing images from Landsat. In Section 4 we present time series of water storage changes from GRACE satellite gravimetry. The temporal evolution of the mass changes with respect to the development of the lake geometry is discussed in Section 5, and conclusions from the work are provided in Section 6.

2. Changes in water level

The present appearance of the Aral Sea is not unique in its entire history. The paleo-variability of the Aral Sea was characterized by similar fluctuations in the past forced by natural climate changes. But in contrast, the continuous severe decline of the lake level that started in the 1960s is primarily caused by

strong anthropogenic consumption (Boroffka et al., 2005; Zavialov 2005). Figure 1 shows a time series of the mean lake level in yearly intervals since 1780. Data between 1780 and 1960 (pre-desiccation time) has been collected by Rogov (1957), data between 1911 and 2006 has been published in the frame of the INTAS-0511 REBASOWS project (Nachtnebel et al., 2006).

Fig. 1 here

The curve shows a decline of a few meters twice in the 19th century. During the first half of the 20th century the lake surface remained on a stable height. But since the beginning of the 1960s an immense decrease of the lake level due to the expansion of an irrigation project that drained out its two major tributaries can be observed (Micklin, 1988). In 1986 the lake was split into two parts: the smaller North Aral Sea and the larger South Aral Sea. The South Aral Sea continued its shallowing while the level of the North Aral Sea fluctuated with the construction, demolition and re-construction of a dam between the two parts of the Aral Sea. In the 180 years between 1780 and 1960 the lake had experienced only fluctuations of smaller than 5 meters. On the contrary it faced a decline of more than 25m over the past 50 years.

In this study we focus on the quantitative changes of the Aral Sea from spring 2002 until autumn 2011. Water level changes were determined from radar altimetry measurements from Jason-1, Jason-1 extended mission (EM), Jason-2, Envisat, Envisat extended mission (EM) and GFO, complemented by laser altimetry measurements from Icesat (for details see Table 1). The radar altimeter satellites provide a significantly higher temporal resolution (10-35 days) than Icesat (91 days). On the other hand the laser altimeter Icesat provides more precise observations because of its smaller footprint (70-90m) and higher frequency. Data were obtained from the Open Altimetry Data Base (OpenADB) of the German Geodetic Research Institute (DGFI) at http://openadb.dgfi.badw.de/.

Tab. 1: Altimetry data used in this study**.**

Satellite	Agency	R.r.a (*) Diameter	Revisit	Pass Numbers	From	Until	Source
JASON-1	CNES,NASA	16 cm	10 days	142, 107, 218	January 2004	January 2009	http://sealevel.jpl.nasa.gov/missions/jason1/
JASON-2	CNES, NASA	16 cm	10 days	142, 107, 218	July 2008	August 2011	http://sealevel.jpl.nasa.gov/missions/ostm jason2/
JASON-1 extended mission	CNES, NASA	16 cm	10 days	107	February 2009	August 2011	http://sealevel.jpl.nasa.gov/newsroom/spotlights/index.cfm?FuseAction=ShowNews&NewsID=338
Envisat, RA2	ESA	20 cm	35 days	0126, 0211, 0797, 0253, 0711, 0167, 0670, 0625, 0584	January 2004	July 2010	http://envisat.esa.int/earth/www/object/index.cfm?fobjectid=3774
Envisat extended mission	ESA	20 cm	30 days	0139, 0369, 455, 0685, 0730, 0771	October 2010	July 2011	http://www.esa.int/esaCP/SEM08O1OWUF_index_0.html
GFO	US Navy	16 cm	17 days	253, 156, 339, 425	January 2004	September 2008	http://ibis.grdl.noaa.gov/SAT/gfo/bmpcoe/default.htm/
IceSAT	NASA	18 cm	91 days	2660, 0799, 0561, 0458, 0293, 0696, 0055, 0531, 0190	January 2004	October 2009	http://icesat.gsfc.nasa.gov/icesat/

(*) R.r.a = Retro reflector array

Heights are provided with respect to the geoid EGM2008 (Palvis et al., 2008). All observations were corrected for atmospheric delay and geophysical effects using calibration models and/or onboard measurements for ionosphere, dry troposphere, wet troposphere, and solid Earth tides (see Fu & Cazenave, 2001 for details). Model based ionospheric corrections were applied since corrections based on onboard radiometer data are not applicable over inland water bodies. All above mentioned missions except GFO are equipped with a dual frequency system (Ku and C band) from which respective corrections can be modeled. GFO observations were corrected by data from Global Ionosphere Maps (GIM; Schaer et al., 1996). Wet tropospheric corrections are based on ECMWF (European Centre for Medium-Range Weather Forecasts) data except for Jason 1 which was corrected by data from the JMR (Jason-1 Microwave Radiometer) following Brown (2010). An ultra stable oscillator range correction was applied to Envisat observations. Altimetry observations between December and March could be

affected by errors due to ice cover, since the reflection of the signal on ice differs significantly from reflections on open water (Kouraev et al., 2008). To prevent a contamination of the measurements by reflections from land, only observation points with a distance of more than 5 km from the coast were considered. For this purpose twice a year in spring and autumn water masks generated from Landsat data were applied in order to account for the continuous changes of the coastline. As a consequence less reliable altimetry observations are available (Fig. 2) during periods when the horizontal extent of the lake is small.

The east basin of the Aral Sea, for example, was observed in October 2009 by Icesat for the last time before the mission was retired in the same month. For almost half a year (November 2009 – June 2010) no observations from the east basin are available, while it has been observed very well in earlier years by Envisat, GFO, Icesat and Jason1 (Figs. 2 and 3). After October 2010 Envisat-EM was capable of providing some measurements over that part of lake (Fig. 2, right), however due to problems of Envisat over ice-covered regions only few of these observations are reliable. The west basin is inadequately observed especially in its northern part mainly because fewer passes are available in this region (Envisat/Envisat EM and few Icesat observations) and furthermore the lake is so narrow that most of the data points are rejected due to the 5 km criteria. The southern part of the west basin was well observed by GFO, Envisat and Icesat until 2010, but afterwards only observations from Jason1-EM and very few reliable data points from Envisat-EM are available. In general all basins have been sparsely observed by altimetry for the last three years, firstly because fewer missions are available (i.e. only Jason2, Jason1-EM and few Envisat-EM observations) and secondly because of the smaller extent of the lake.

Fig. 2 here

With these limitations, a multi-mission altimetry data combination provides maximum information on the development of the lake level. A best possible harmonization was reached between the different missions by selecting similar calibration models as far as feasible. An additional cross calibration of the range bias was applied by estimating a constant offset of each mission relative to the orbit of Topex/Posidon (Bosch & Savcenko, 2007). Inter and intra mission crossover analysis was done over the east and north basin where the passes of GFO, Icesat, Envisat and Jason1 are close enough to compare the calibrated data with respect to each other. A nominal ground track on geographically fixed segments was maintained by aggregating all observations within a 10 km radius to a mean value per cycle.

Fig. 3 here

Figure 3, shows the results of our multi-mission altimetry analysis for the different basins of the Aral Sea. Here we approximate the lake level of each basin as a flat surface, i.e. we do not distinguish between the various locations of the footprints within an individual basin. The observations show the picture of one of the worst environmental catastrophes by illustrating the drastic drop of the water level in the west and east basins. The observations of all missions agree very well to each other. Besides the trends all curves feature clear seasonal signals. Data from altimetry agree quite closely to annual in-situ observations from the previously mentioned INTAS-0511 REBASOWS project (Nachtnebel et al., 2006) and from observations collected during expeditions on the west basin (Zavialov 2010). In-situ observations are available until 2006 (North Aral Sea), 2007 (west basin) and 2009 (east basin) with one data point per year. Although an offset of about 50-70 cm exists between the altimetry missions and

157 in-situ observations, they follow the same trend. The reason for the offset could be a difference in the
158 reference systems since all altimetry measurements refer to EGM2008 while the in-situ observations
159 refer to the mean seal level of the Baltic Sea. Furthermore, the in-situ water levels are given as one data
160 point per year with (except for the west basin) no information about the time of acquisition.
161
162 The most drastic changes in water level were observed in the South Aral Sea, i.e. the east and west
163 basin. The east basin suffered nearly 3.5 m decline in eight years (2002-2009) while the level of the
164 west basin fell by about 4 m. The curve of the North Aral is significantly different due to the
165 construction of the Dike Kokaral dam in October 2005. After its completion the water level increased
166 by about two meters within only half a year. The inflow from the Syr Darya revived the North Aral and
167 led to a rather stable water level since 2006 with fluctuations of less than 1 m. On the other hand the
168 construction of the dam accelerated the desiccation in the other two basins from 2006 as the dam cut off
169 the South Aral Sea from the tributary Syr Darya. Only in the case of overflow of the North Aral Sea
170 water from this river is diverted into the southern basins. The east basin reached the stage of drying up
171 of most of its area in 2009 (which led to the previously mentioned non-availability of reasonable
172 altimetry data until the lake level started to rise again in 2010). Jason-2 observations indicate that the
173 lake had regained more than 0.5 m by the last seven months of 2010 as a consequence of exceptionally
174 strong inflow from the Amu Darya (see Section 5). This increase of the lake level was followed by the
175 normal seasonal decline in summer 2011. A clear seasonal variability of the lake level due to season-
176 dependent inflow and evaporation is obvious for all basins.
177

3. Changes in the lake surface area

Changes in the coastline of the Aral Sea and therewith of the horizontal lake extent were derived from Landsat multi-spectral remote sensing data (30 m spatial resolution) for a month in spring and autumn every year from 2002 to 2011. Due to the high computational effort of the data analysis we restricted ourselves to two snapshots per year. However, during periods of special interest (see Fig. 5 and Section 5) the coastline was also computed for some additional months in order to get a better insight into the temporal development of the lake extent. Precision and terrain corrected Landsat images were obtained from USGS Earth Explorer website (http://earthexplorer.usgs.gov). Three Landsat images were combined in order to cover the entire area of the Aral Sea. Due to the presence of clouds and data problems in the course of the image acquisition it was not always possible to obtain an image combination with all images acquired within one month. In such cases images of two subsequent months were taken into account (e.g. for the spring season images from April and March, or for the autumn season images from October and September) in order to produce a complete picture of the horizontal lake geometry.

Water absorption bands, i.e. short wave infra-red (SWIR), near infra-red (NIR) and middle infra-red (MIR) bands of Landsat images were stacked. The three Landsat images per date were mosaicked to a complete map of the Aral area. The mosaicked images were then classified with a maximum likelihood supervised classifier (MLC) to generate a water mask. The MLC was trained by the a priori knowledge of the spectral signature of water and non water classes. In the course of this training step the variance/covariance matrix of the training site classes is calculated. Based on Bayesian statistics the probability of a pixel belonging to the class is estimated. A pixel is assigned to the class which has the highest probability. Accuracy assessments of the classified images were done by a confusion/error

matrix formed by reference data in columns and classified data in rows. In this study an original image was used in place of reference data, and pixels from stratified random sampling were verified visually. The producer accuracy for all classified images was found to be between 85 to 90%. This value indicates how well a certain area is classified. It is computed by dividing the number of pixels of the reference class that were correctly classified with the total number of pixels of that reference class. The classified image was then transformed into a boolean image in order to obtain the water mask.

A few Landsat images feature striping errors due to a failure of the scan line corrector (SLC) that led to a permanent data loss (http://landsat.usgs.gov/products_slc_off_data_information.php). In the used spectral bands (bands 3, 5 and 7) a SLC gap has a maximum width of 14 pixels. In order to avoid negative effects on the extracted water boundary by applying a destriping algorithm (e.g., a low pass convolution filter) we preferred to fill the scan gaps with data for the same location from the closest cycle. In most of the cases this substitution of data decreased the scan line gap to 2-3 pixels, which can be filled by simple low pass filter without a strong effect on the boundary lines. In few severe cases, when a close cycle was not available (e.g. due to clouds), the classified images have been digitized and edited manually to generate a polygon vector layer. The area under water was subsequently calculated from each of the generated seasonal masks. Figure 4 shows the drastic changes in the extent of the Aral Sea during the analyzed period. Between spring 2002 and autumn 2009 a clear signal of desiccation is visible. This decline is followed by a significant increase of the lake extent reaching its maximum revived stage between autumn 2010 and spring 2011. This period is followed by substantial decline until the end of our data set.

Fig 4 here

During spring the area under water is generally larger due to substantial inflow of melt water from the tributaries of the lake (Kravtsova, 2005) and relatively low evaporation during the winter months. On the contrary, strong evaporation during the summer months and a cooling of the lake towards autumn lead to lower water levels in the second half of the year. Figure 5 shows the temporal evolution of the lake surface area with respect to spring 2002 for the entire lake and separately for its sub-basins. The seasonal changes of the lake surface area are obvious in all curves.

Fig 5 here

In 2002 the Aral Sea consisted of two completely separated sub-basins, the North Aral Sea and the larger South Aral Sea. The latter was later divided into two parts (west and east basin), connected by a narrow channel. The shrinking rate of the Aral Sea is largest in the east basin, while a negative trend can also be seen for the west basin. The curve for the surface area of the North Aral Sea shows a stable geometry with normal seasonal variations after an increase due to the construction of the dam in 2005/2006. Thus it matches the characteristics of the corresponding curve of the lake level (Fig. 3). The west basin suffered comparatively little loss in area over the first eight years of our analysis (2002-2009), but it also does not show any significant increase in size in 2010 where the signal of re-flooding can clearly be observed in the east basin. This relative stability of the area of the west basin can be explained by its steeper coastline (Zavialov, 2005). Some inflow from ground water (Jarsjo, 2004) also compensates the water loss by evaporation to a certain extent. Overall, the east basin, being quite shallow (Roget et al., 2009), experienced the largest changes of coastline and surface area over the analyzed period. After the erection of the Dike Kokaral dam it was cut-off from its former tributary Syr

247 Darya (see above). An especially rapid decrease of the surface area of the east basin was observed in
248 2006. This strong reduction of the lake size can be attributed to increased evaporation due to high
249 temperature anomalies between 1-3°C and very dry conditions in the region during this year (Arguez,
250 2007) in combination with almost no water inflow from the Amu Darya in 2006 (see Fig.8).
251
252 The Aral Sea as a whole suffered 62% area loss within eight years (spring 2002 - autumn 2009), out of
253 which the east basin contributes the largest fraction: With respect to its extent in spring 2002 only 6%
254 were left in autumn 2009. With the shrinking of the lake salt crusts of up to 2-10 km width formed
255 along the coast (Kravtsova & Tarasenko, 2010). The boundary of this moist salty surface changes its
256 shape frequently, especially in the shallow east basin. Once the crust dries up it is eroded by strong
257 winds that are prevalent in the region. As a consequence the topography of the land that has fallen dry
258 changes quickly due to the salty dust storms. This explains why during the refilling in April 2010 the
259 lake did not regain a similar same shape as it had before although it nearly reached the same surface
260 area (52% of the area of spring 2002) as it had in autumn 2008 (Fig. 5).
261

4. Mass changes in the region of the Aral Sea observed from by GRACE

Ongoing changes of sea surface area and height are associated with strong variations of water mass being stored in the individual basins. These storage changes map into satellite-based observations of temporal variations of the Earth's gravity field as they are provided from the dedicated satellite gravity field mission GRACE (Gravity Recovery And Climate Experiment) (Tapey et al., 2004; Wahr et al., 2004). Several previous studies have shown the potential of GRACE observations for the estimation of hydrological storage variations in continental regions (e.g., Ramillien et al., 2008; Schmidt et al., 2008; Seitz et al., 2008). Due to the characteristics and height of the GRACE orbit, meaningful results are restricted to regions not smaller than 200.000 km^2 (Swenson and Wahr, 2007). At this scale the maximum temporal resolution amounts to approximately one month. The coarse resolution of GRACE prevents the assessment of water storage for each individual sub basin of the Aral Sea from satellite gravimetry. Instead we provide quasi-monthly estimates of water mass variability within the region confined by the minimum and maximum latitudes of 43.5 °N and 47.5 °N and by the minimum and maximum longitudes of 58 °E and 62 °E respectively. This quadrangle comprises the area of the Aral Sea in its historic dimensions and thus the entire region affected by desiccation over the past decades. Its surface area amounts to 220.000 km^2. Even though this study region is much larger than the present surface of the Aral Sea it can be assumed that the prominent part of mass variations on long (i.e. inter-annual) time scales originates from the long-term storage change of water in the Aral Sea. Other sources of water storage variations in its surrounding area (e.g. variations in groundwater, soil moisture or snow cover) are expected to predominantly result in seasonal variations. Therefore we interpret the GRACE signal reduced by seasonal components as an approximation of the long-term water storage in the Aral Sea.

Our GRACE analyses are based on quasi-monthly sets of spherical harmonic coefficients of the Earth's gravity field (GRACE Level-2 data) as provided by the GFZ German Research Centre for Geosciences and the Center for Space Research (CSR), USA, in its well-established latest releases RL04 (Flechtner et al., 2010; Bettadpur, 2007). Mass redistributions on sub-monthly time scales (e.g. due to Earth and ocean tides, atmospheric pressure variations and ocean circulation) would lead to alias effects of the gravity estimates from GRACE in the course of the inversion of the GRACE monthly gravity field solutions. Therefore, those effects are reduced from the GRACE observations already during pre-processing using respective background models; see Flechtner (2007) for details. For continental non-polar regions the largest part of the remaining gravity field changes provided in the monthly Level-2 GRACE products is assumed to reflect mass redistributions within the continental hydrology.

We analyze monthly GRACE gravity field solutions covering the time span from April 2002 (CSR)/August 2002 (GFZ) until July 2011. Due to orbit maneuvers and data problems, few individual months are unavailable. Variations of the gravity field are computed with respect to a long-term mean, i.e. the mean GRACE gravity field over the entire time span. In a spherical harmonic synthesis the coefficients of the residual monthly solutions complete up to degree and order 60 are converted into geographical grids of so-called equivalent water height (EWH) variations (Wahr et al., 1998). EWHs mean an idealized representation of surface mass densities in terms of a thin water layer that needs to be added to (or removed from) the Earth's surface. By expressing GRACE-derived gravity field changes in changes of the thickness of a water layer, it is implicitly assumed that the total observed gravity signal is caused by variations of water storage. The accuracy of the EWH estimates from GRACE is assumed to be 1-2 cm, depending on region and size of the study area (Swenson et al., 2003; Wahr et al., 2006).

Mission-specific errors in the GRACE Level-2 data that show up as meridional stripes in maps of gravity field variations have to be treated in the course of the conversion of the gravity field coefficients into EWH variations. Those errors emerge from satellite orbit characteristics and measurement limitations which result in an in-ability to separate spherical coefficients at all degrees and orders, in particular near orders of resonant coefficients. In addition un-modelled mass fluctuations on sub-monthly timescales (see above) cause high-frequency aliasing. In order to minimize the effects of these errors on the solutions of monthly EWH variations algorithms for smoothing and destriping are applied. In our study we follow the widely used procedures described by Swenson and Wahr (2006) and Wahr et al. (1998), in which correlated errors in the gravity field coefficients are reduced by a least squares polynomial filter and noisy short wavelength components are smoothed using an isotopic Gaussian filter with a half-width of 300 km. As a consequence of Gaussian smoothing, leakage effects from strong mass signals outside of our region of interest emerge (Baur et al., 2009; Swenson and Wahr, 2007). In order to eliminate this contamination of the mass signal within the Aral region, leakage effects from the surrounding area are forward modelled using the WaterGAP Global Hydrology Model (WGHM; Döll et al., 2003) on which the same Gaussian filter is applied. The resulting leakage signal is subsequently reduced from the GRACE signal in the study area. A final correction step accounts for the attenuation of the mass signal as a consequence the spherical harmonic truncation at degree and order 60 and the Gaussian smoothing. In order to derive meaningful values, the GRACE signal amplitude needs to be rescaled. Following the procedure outlined by Swenson and Wahr (2007) a simulated water layer of 1 cm within the study region was developed into spherical harmonic coefficients up to degree and order 60. Taking into account the filter procedure described above, these coefficients were applied in a spherical harmonic synthesis in order to reconstruct the water height in the study region. The

relation of the simulated and the mean of the reconstructed water height (i.e. 1 cm vs. 0.38 cm) let us conclude that the GRACE signal is attenuated by a factor of 2.6. Therefore each value of the grid is multiplied by this factor. We compare the result of our own GRACE Level-2 data analysis from GFZ and CSR with a result based on publicly available spherical harmonic coefficients based on GFZ RL04 data that have been de-correlated using the filter DDK1 after Kusche et al. (2009). These coefficients are provided by the International Centre for Global Earth Models (ICGEM) at http://icgem.gfz-potsdam.de/ICGEM.

Fig 6 here

Figure 6 displays the rescaled results of the GRACE analysis in the study area. Water mass variations (provided in units of km^3) are derived by multiplying the surface area of the region with monthly averages of the gridded EWH residuals. The dashed curves show the complete GRACE signal in quasi-monthly time steps from the GFZ, CSR and DDK1 solutions respectively. The bold solid curve represents the mean of the three solutions and the thin solid curve is the long-term component of this mean curve, i.e. a composite seasonal cycle is removed. The results of the two approaches based on the GFZ data agree very well whereas the curve computed from CSR data shows larger discrepancies especially during the second half of the study period. This lets us conclude that the spread of the results is dominated by the different processing strategies at GFZ and CSR rather than on the different approaches for the conversion of the Level-2 data into EWH variations.

Besides a pronounced annual cycle the GRACE signal indicates a clear long-term mass loss between 2005 and 2008. The effect of the previously mentioned anomalous warm and dry conditions of the year

2006 (cf. Section 3) can also be identified in the observations of GRACE that indicate a strong decrease of water storage during summer 2006. From the end of 2009 until mid-2010 the GRACE observations indicate a strong increase of mass in the Aral region which is followed by a rapid decline to the previous level.

Between mid-2005 and the end of 2008 approximately 60 km^3 of water mass were lost in the study area. In a rough calculation we relate this mass loss to a change of the water level given the mean surface areas of the lake in 2005 (around 18.000 km^2) and in 2009 (about 10.000 km^2) (cf. Fig. 5). For simplicity we take 14.000 km^2 as a mean value of the lake's surface area during this period. For this horizontal extent the observed mass loss of 60 km^3 of water corresponds to a sea level change of about 4.3 m which coincides well with the observations from satellite altimetry (Figs. 5 and 6). Since the actual lake geometry is much more complex this estimate can of course only be viewed as a rough plausibility check. Due to its integrative nature the GRACE signal also contains contributions from other mass changes (e.g. due to surface or groundwater variations) in the proximity of the lake whose magnitude and origin are widely unknown. Especially during periods, when the spatial extent of the lake is small (i.e. when the largest part of our GRACE study area is not covered by water), the relative contribution of mass changes from other sources is increased. Due to the limited spatial resolution of GRACE this problem cannot be solved by a stepwise adaptation of the size of the study area to the respective extent of the lake. For a more precise estimation of the contribution of the lake water change to the GRACE signal volume variations of the lake can be computed considering its actual bathymetry (Crétaux et al, 2005). But since the bathymetry of the lake has been shown to be subject to considerable changes resulting from the previously mentioned dust storms such computations are a challenging task for future research (see Section 6) and beyond the scope of the present paper.

5. Discussion:

Figure 7 shows the mean curve of the GRACE solutions with the temporal change of the surface area of the entire Aral Sea (bold solid line from Fig. 5). In this figure only values for those GRACE months are displayed for which the surface area has been computed. Both curves clearly resemble each other in terms of inter-annual and seasonal variations and the correlation coefficient between the curves amounts to 0.74. The characteristics of both curves match well between 2004 and 2008, but the agreement is less good during the first two and the last two years of our analysis. While the minima of the GRACE curve in the autumn of 2008, 2009 and 2010 reach very similar values, the curve of the surface area as well as the time series of the water level (see Fig.3) feature a clear minimum in autumn 2009. However it has to be kept in mind that GRACE is sensitive not only for variations of water mass within the lake but also for the integral effect of all mass changes in the surrounding of the Aral Sea.

In the Priaralie region, i.e. the region compassing the mouths of the two rivers Amu Darya and Syr Darya, a significant fraction of the incoming water is diverted before it reaches the lake. This holds especially for the region of the very large Amu Darya delta. A part of the diverted water subsequently evaporates or is accumulated as groundwater around the Aral Sea (Nezlin et al., 2004). In either case its positive or negative mass effect affects the GRACE signal in our study region but it is not reflected in the observations of the lake geometry.

Fig 7 here

In order to study the effect of the surrounding area, data on the water delivery from both rivers into the

Aral Sea and its delta were analyzed that is provided by the INTAS-0511 REBASOWS project (Nachtnebel et al., 2006) on the website http://www.cawater-info.net. In Fig. 8 variations of the lake surface area and the mass changes from GRACE are compared with in-situ water discharge observations from Amu Darya and Syr Darya. Discrepancies between the curves of the surface area and the mass signal occur mainly during periods of strong inflow from the Amu Darya into the Aral Sea.

Fig 8 here

GRACE shows a minimum of water mass by the end of 2008. During this time almost no discharge was observed at both rivers. Some discharge of Syr Darya in the beginning of 2009 increased the water level of the North Aral Sea that had reached its minimum stage by the end of 2008 (Fig. 3). In summer 2010 an abnormally increased discharge into the Aral Sea was observed at Amu Darya. This flood led to the strongest increase of the lake level and extent during our study period. A time lag of few months is obvious between the GRACE curve and the lake water extent. Again this can be explained by the sensitivity of GRACE for signals from the adjoining region. The usual strong intra-annual shrinking of the lake (i.e. lower water levels in autumn than in spring) cannot be observed in 2010 because of the exceptional water inflow from Amu Darya during summer 2010. The lake has experienced a similar anomaly of the annual cycle in 2003 where relatively strong inflow (the second largest amount in our study period) also attenuated the usual minimum in autumn. Also here a comparable phase difference between GRACE and the lake extent is visible.

In general there is a very good agreement between the curve of the discharge measured at the Syr Darya gauge station and the GRACE signal. Since the GRACE study area covers a large part of the region east

of the Aral Sea through which the Syr Darya is passing, GRACE is sensitive to the water transport of the river and hydrological processes (evaporation, infiltration, water management) in this region. In particular during the first seven years the inter-annual signal component of both time series (i.e. the increase from 2002 to 2005 and the decrease between 2005 and 2008) matches in both curves. For the last years of our analysis the GRACE time series has mainly been influenced by the exceptional water transport from Amu Darya.

In 2010 GRACE observed a decrease in mass between April and September. On the other side a significant refilling of lake was ongoing during this period due to the strongest inflow from the Amu Darya during the whole study period. Between August and November 2010 the discharge curve dropped back to its previous low level. The GRACE curve precedes the discharge curve of Amu Darya by two to three months. This can also be seen in other years with strong discharge from Amu Darya (e.g. 2003). Since the Amu Darya is passing through the Kara-Kum desert a large amount of surface water is lost due to seepage which is accompanied by the accumulation of groundwater along the river bed and around the Aral Sea (Nezlin et al., 2004). It is assumed that in the case of strong runoff from Amu Darya aquifers around the Aral Sea are filled before the water reaches the lake and thus influence the observations of GRACE.

Fig 9 here

Figure 9 relates the lake area to mass changes from GRACE. Data points are taken from Fig. 7. The line shows a best fit estimate that has been computed in a least squares adjustment procedure. A statistically significant linear relationship indicates the link between the GRACE mass estimates and the Aral Sea water surface at the inter-annual scale.

6. Conclusions

The combination of multi-satellite data of the Aral region allows for a comprehensive study of the hydrological conditions in this area. Satellite altimetry, remote sensing, and satellite gravimetry provide information on various aspects of the ongoing storage changes in the Aral Sea and its basins that are largely related to anthropogenic activities. While satellite altimetry and remote sensing data allow for an accurate assessment of a three dimensional geometrical change of the lake surface, satellite gravimetry is capable of observing the related variations of water mass. Even though the spatial resolution of geometrical and gravimetrical observations is very different, both types of observations provide valuable and unique information on different aspects of the hydrological situation.

The observations revealed that the impact of desiccation on the lake geometry is most severe in the comparatively shallow east basin. The completion of the Dike Kokaral dam resulted in a splitting of the smaller North Aral Sea from the larger South Aral Sea. While the dam led to a stabilization of the water level of the north basin, the south basin suffered an increased desiccation since it was cut off from the tributary Syr Darya, and the water discharge from the Amu Darya was too low (especially during 2006-2009; see Fig. 8) to compensate for the high rate of evaporation due to its very large size. Since the deeper west basin is characterized by a steeper coastline, the horizontal shrinkage of the west basin is comparatively low while the water level varies significantly. The patterns of desiccation and subsequent refilling observed by the geometrical observation techniques are also clearly visible in the GRACE satellite gravimetry data. However due to the small size of the lake a direct comparison of observed mass variations and the lake geometry is very difficult since the GRACE signal is strongly affected by the variability of the water mass in the adjoining area.

Therefore we aim at an independent computation of mass variations from water volume changes in a

next step of our project. In a geometrical approach time-variable masks of water surface extent from Landsat shall be intersected with a high-resolution DEM, using satellite altimetry as vertical constraint. This way volume changes from geometrical observation techniques and mass change from gravity field observations can be compared qualitatively which will also allow for an improved assessment of the influence of hydrological mass variations in the proximity of the lake. The study has shown that all applied data sets correspond well with respect to their temporal development. Therefore multi-satellite approaches can be seen as a very promising method for the analysis of hydrological processes also in regions that are poorly monitored by in-situ observations.

Acknowledgements:

The authors acknowledge the financial support by the WILLPower Erasmus Mundus Cooperation Window and by the International Graduate School of Science and Engineering (IGSSE) of the Technische Universität München, Germany. Further we thank the anonymous reviewers for constructive remarks on the manuscript that led to a substantial improvement of the paper.

References:

Arguez, A. (Ed.), 2007. State of the Climate in 2006, *Bull. Am. Meteorol. Soc*., 88, 135pp, Washington, USA.

Baur, O., Kuhn, M. & Featherstone, W., 2009. GRACE-derived ice-mass variations over Greenland by accounting for leakage effects, *J. Geophys. Res*., 114, B06407, doi:10.1029/2008JB006239.

Becker, M., Llovel, W., Cazenave, A., Güntner, A. & Crétaux, J-F, 2010. Recent hydrological behavior of the East African great lakes region inferred from GRACE, satellite altimetry and rainfall observations, *Comptes Rendus Geoscience*, 342, 3, 223-233. doi:10.1016/j.crte.2009.12.010.

Bettadpur, S., 2007. Gravity Recovery and Climate Experiment Level-2 Gravity Field Product User Handbook, *GRACE 327-734, CSR Publ. GR-03-01, Rev 2.3*, 19pp., University of Texas at Austin, USA.

Birkett, C.M., 1995. The contribution of TOPEX/POSEIDON to the global monitoring of climatically sensitive lakes, *J. Geophys. Res.*, 100 (12), 25179-25204.

Boroffka, N.G.O., Obernhänsli, H., Achatov, G.A., Aladin, N.V., Baipakov, K.M., Erzhanova, A., Hörnig, A., Krivonogov, S., Lobas, D.A., Savel'eva, T.V., & Wünnemann, B., 2005. Human Settlements on the Northern Shores of Lake Aral and Water Level Changes, *Mitigation and Adaptation Strategies for Global Change*, 10 (1), 71-85, doi:10.1007/s11027-005-7831-1.

Bortnik, V.N., 1999. Alteration of water level and salinity of the Aral sea, in Glantz, M (Ed.), *Creeping Environmental Problems and Sustainable Development in the Aral Sea Basin*, Cambridge University Press, Cambridge, UK, 47–65.

Bosch, W., Savcenko, R., 2007. Satellite Altimetry: Multi-Mission Cross Calibration, in Tregoning, P., Rizos, R. (Eds.), *Dynamic Planet IAG Symposia* 130, 51-56, doi: 10.1007/978-3-540-49350-1_8.

Brown, S., 2010. A Novel Near-Land Radiometer Wet Path-Delay Retrieval Algorithm: Application to the Jason-2/OSTM Advanced Microwave Radiometer, *IEEE Trans. Geosc. Remote Sens.*, 48, 4.

Calmant, S., Seyler, F., & Cretaux, J.F., 2009. Monitoring Continental Surface Waters by Satellite Altimetry, *Surv. Geophys.*, 29 (4-5), 247-269, doi:10.1007/s10712-008-9051-1.

Cazenave, A., Bonnefond, P., Dominh, K., & Schaeffer, P., 1997. Caspian sea level from Topex-Poseidon altimetry: Level now falling, *Geophys. Res. Lett*., 24 (8), 881-884, doi:10.1029/97GL00809.

Crétaux, J.F., Calmant, S., Romanovski, V., Shabunin, A., Lyard, F., Bergé-Nguyen, M., Cazenave, A., Hernandez, F., & Perosanz, F., 2008. An absolute calibration site for radar altimeters in the continental domain: Lake Issykkul in Central Asia, *J. Geodesy*, 83 (8), 723-735, doi:10.1007/s00190-008-0289-7.

Crétaux, J.F., Kouraev, A.V., Papa, F., Bergé-Nguyen, M., Cazenave, A., Aladin, N., & Plotnikov, I.S., 2005. Evolution of Sea Level of the Big Aral Sea from Satellite Altimetry and Its Implications for Water Balance, *J. Great Lakes Res.*, 31 (4), 520-534, doi:10.1016/S0380-1330(05)70281-1.

Döll, P., Kaspar, F., & Lehner B., 2003. A Global Hydrological Model for Deriving Water Availability Indicators:

519 Model Tuning and Validation, *J. Hydrology*, 270 (1-2) 105-134, doi:10.1016/S0022-1694(02)00283-4.

520 Flechtner, F., Dahle, C., Neumayer, K.H., König, R. & Förste, C., 2010. The Release 04 CHAMP and GRACE
521 EIGEN Gravity Field Models, in Flechtner, F., Mandea, M., Gruber, T., et al., (Eds.), *System Earth via*
522 *Geodetic-Geophysical Space Techniques*, Springer, Berlin, 41-58, doi: 978-3-642-10228-8.

523 Flechtner, F., 2007. Gravity Recovery and Climate Experiment AOD1B product description document for
524 product releases 01 to 04. Tech. Rep. GRACE327-750, Rev. 3.1, GFZ Potsdam, Germany.

525 Frappart, F., Papa, F., Famiglietti, J.S., Prigent, C., Rossow, W., & Seyler,, F., 2008. Interannual variations of
526 river water storage from a multiple satellite approach: A case study for the Rio Negro River basin. *J. Geophys.*
527 *Res*., 113, D21104, doi:10.1029/2007JD009438.

528 Froebrich, J. & Kayumov, O., 2004. Water management aspects of Amu Darya, in Dying and Dead Seas
529 Climatic Versus Anthropic Causes, in Nihoul et al. (Eds.), *NATO Science Series IV: Earth and*
530 *Environmental Sciences*, 36, 49-76, Kluwer Academic Publishers, Dordrecht, The Netherlands.

531 Fu, L. & Cazenave, A., 2001. *Satellite altimetry and Earth sciences: a handbook of techniques and*
532 *applications*, 464 pp, Academic Press, London, UK.

533 Getirana, A.C.V., Bonnet, M.P., Calmant, S., Roux, E., Rotunno-Filho, O.C., & Mansur, W.J., 2009. Hydrological
534 monitoring of poorly gauged basins based on rainfall-runoff modeling and spatial altimetry, *J. Hydrology*, 379
535 (3-4), 205-219, doi:10.1016/j.jhydrol.2009.09.049.

536 Güntner, A., 2008. Improvement of Global Hydrological Models Using GRACE Data, *Surv Geophys*, 29 (4-5),
537 375-397, doi:10.1007/s10712-008-9038-y.

538 Jarsjo, J., 2004. Groundwater discharge into the Aral Sea after 1960, *J. Marine Sys*., 47(1-4), 109-120,
539 doi:10.1016/j.jmarsys.2003.12.013.

540 Kravtsova, V.I., 2005. The Aral Sea and Coastal Zone Degradation: Monitoring by Space Images, in *Proceedings*
541 *of 31st International Symposium on Remote Sensing of Environment*, Saint Petersburg, Russia.

542 Kravtsova, V.I., & Tarasenko, T.V., 2010. Space monitoring of Aral Sea degradation, *Water Res.*, 37(3), 285-296,
543 doi:10.1134/S0097807810030036.

544 Kouraev, A.V., Shmaraev, M.N., Buharizin, P.I., Naumenko, M.A., Crétaux, J.F., Mognard, N., Legrésy, B., &
545 Rémy, F., 2008. Ice and Snow Cover of Continental Water Bodies from Simultaneous Radar Altimetry and
546 Radiometry Observations, *Surv. Geophys.*, 29(4-5), 271-295, doi:10.1016/j.jmarsys.2008.03.016.

547 Kusche, J., Schmidt, R., Petrovic, S. & Rietbroek, R., 2009. Decorrelated GRACE time-variable gravity
548 solutions by GFZ, and their validation using a hydrological model. *J. Geodesy*, 83(10), 903-913, doi:
549 10.1007/s00190-009-0308-3.

550 Micklin, P.P., 1988. Desiccation of the Aral Sea, a water management disaster in the Soviet Union, *Science*, 241,
551 1170–1176.

552 Morris, C.S., & Gill, S.K., 1994. Evaluation of the TOPEX/POSEIDON altimeter system over the Great Lakes,
553 *J. Geophys. Res*., 99 (C12), 24527-24539, doi:10.1029/94JC01642.

554 Nachtnebel H.P., Holzmann H., Dukhovny V., Sorokin A., Roschenko Y., et al., 2006. *The rehabilitation of the*
555 *ecosystem and bioproductivity of the Aral Sea under conditions of water scarcity*, Final report of the INTAS
556 project 0511 REBASOWS, 75 pp., Vienna, Austria.

557 Nezlin, N., Kostianovy, A. & Lebedev, A., 2004. Interannual variations of the discharge of Amu Darya and Syr
558 Darya estimated from global atmospheric precipitation. *J. Marine Systems*, 47, 67-75.

559 Papa, F., Güntner, A., Frappart, F., Prigent, C., & Rossow W., 2008.Variations of surface water extent and water
560 storage in large river basins: A comparison of different global data sources, *Geophys. Res. Lett.*, 35, L11401,
561 doi:10.1029/2008GL033857.

562 Prigent, C., Papa, F., Aires, F., Rossow, W.B., & Matthews, E., 2007. Global inundation dynamics inferred from
563 multiple satellite observations, 1993–2000, *J. Geophys. Res.*, 112, D12107, doi:10.1029/2006JD007847.

564 Pavlis, N.K., Holmes, S.A., Kenyon, S.C. & Factor, J.K., 2008. An Earth Gravitational Model to degree 2160:
565 EGM2008, *Geophys. Res. Abstr.*, 10, EGU2008-A-01891.

566 Ramillien, G., Frappart, F., Cazenave, A., & Guntner, A., 2005. Time variations of land water storage from an
567 inversion of 2 years of GRACE geoids, *Earth Planetary Sci. Lett.*, 235 (1-2), 283-301,
568 doi:10.1016/j.epsl.2005.04.005.

569 Ramillien, G., Famiglietti, J., & Wahr, J., 2008. Detection of Continental Hydrology and Glaciology Signals from
570 GRACE: A Review, Surv. *Geophys.*, 29 (4-5), 361-374, doi: 10.1007/s10712-008-9048-9.

571 Roget, E., Zavialov, P., Khan, V., & Muñiz, M.A., 2009. Geodynamical processes in the channel connecting the
572 two lobes of the Large Aral Sea, *Hydrol. Earth Sys. Sci.* 13(11), 2265–2271, doi:10.5194/hess-13-2265-2009.

573 Rogov M.M., 1957. *Hydrology of the Amudarya Delta*. *Gidrometeoizdat*, 255 pp., Leningrad, Russia (in
574 Russian).

575 Schaer, S., Beutler, G., Rothacher, M., & Springer, T., 1996. Daily global ionosphere maps based on GPS carrier
576 phase data routinely produced by the CODE analysis center, in *Proceedings of the IGS AC Workshop*, Silver
577 Spring, MD, USA.

578 Schmidt, M., Seitz, F., Shum, C.K., 2008. Regional four-dimensional hydrological mass variations from GRACE,
579 atmospheric flux convergence, and river gauge data. *J. Geophys. Res.*, 113, B10402, doi:
580 10.1029/2008JB005575.

581 Seitz, F., Schmidt, M., & Shum, C.K., 2008. Signals of extreme weather conditions in Central Europe in GRACE
582 4-D hydrological mass variations, *Earth Planet Sci. Lett*., 268(1-2), 165-170, doi: 10.1016/j.epsl.2008.01.001.

583 Solomon, S., Qin, D., Manning, M., Chen, Z., Marquis, M., Averyt, K., Tignor M., & Miller H., (eds.), 2007.
584 *Clmate Change 2007: The Physical Science Basis, Contribution of Working Group I to the Fourth Assessment*
585 *Report of the Intergovernmental Panel on Climate Change*, Cambridge University Press, Cambridge, UK.

586 Swenson, S., Wahr, J. & Milly, P., 2003. Estimated accuracies of regional water storage variations inferred from
587 the Gravity Recovery and Climate Experiment (GRACE), *Water Resour. Res.*, 39 (8).
588 doi:10.1029/2002WR001736.

589 Swenson, S. & Wahr, J., 2006. Post-processing removal of correlated errors in GRACE data, *Geophys. Res. Lett.*,
590 33, L08402, doi:10.1029/2005GL025285.

591 Swenson, S., & Wahr, J., 2007. Multi-sensor analysis of water storage variations of the Caspian Sea, *Geophys.*
592 *Res. Lett.*, 34, L16401, doi:10.1029/2007GL030733.

593 Tapley, B., Bettadpur, S., Ries, J., Thompson, P. & Watkins M., 2004. GRACE measurements of mass variability
594 in the Earth system, *Science*, 305, 503-505, doi:10.1126/science.1099192.

595 Wahr, J., Molenaar, M. & Bryan, F., 1998. Time variability of the Earth's gravity field: Hydrological and oceanic
596 effects and their possible detection using GRACE, *J. Geophys. Res*., 103(B12), 30205-30229,
597 doi:10.1029/98JB02844.

598 Wahr, J., Swenson, S., Zlotnicki, V. & Velicogna, I., 2004. Time-variable gravity from GRACE: First results,
599 *Geophys. Res. Lett.*, 31, L11501, doi:10.1029/2004GL019779.

600 Wahr, J., Swenson, S. & Velicogna, I., 2006. Accuracy of GRACE mass estimates, *Geophys. Res. Lett*., 33,
601 L06401, doi:10.1029/2005GL025305.

602 Werth, S., Güntner, A., Petrovic, S., & Schmidt, R., 2009. Integration of GRACE mass variations into a global
603 hydrological model, *Earth Planetary Sci. Lett*., 277(1-2), 166–173, doi:10.1016/j.epsl.2008.10.021.

Zavialov, P.O., 2005. *Physical Oceanography of the Dying Aral Sea*, pp. 22-56 Springer Praxis Book, Chichester, UK.

Zavialov, P.O., 2010. Physical Oceanography of the Large Aral Sea, in Kostianoy, A.G. & Kosarev, A.N. (Eds.), *The Aral Sea Environment: The Handbook of Environmental Chemistry*, 7, 123-145, doi:10.1007/698_2009_4, Springer, Berlin Germany.

Figure captions

Fig. 1: Water level changes in the Aral Sea (1780-2006).

Fig 2: Passes of different satellite altimetry missions over the Aral Sea in (A) March 2002, (B) November 2009 and (C) September 2011.

Fig. 3: Water level changes in the (A) east basin, (B) west basin and (C) North Aral Sea from multi-mission altimetry and in-situ observations.

Fig. 4: Change of the Aral Sea surface area during the study period from Landsat images.

Fig. 5: Percentage change of the surface area of the Aral Sea and its basins with respect to March 2002**.** At this reference, the respective absolute values of the surface extent amounted to 20,370 km^2 (whole Aral Sea), 2,850 km^2 (North Aral Sea), 4,660 km^2 (west basin), and 12,860 km^2 (east basin). The vertical black line indicates the construction of the Dike Kokaral dam.

Fig. 6: Variations of equivalent water mass in the Aral region from GRACE satellite gravimetry. Dashed curves: three different GRACE solutions; solid bold curve: mean of the three solutions; thin solid curve: mean long-term signal (solid bold curve reduced by seasonal variations).

Fig. 7: Mass change in the Aral region from GRACE (solid; left axis) in comparison with the total Aral Sea surface area from Landsat (dashed; right axis) for corresponding epochs.

Fig. 8: Monthly discharge from Amu Darya and Syr Darya into the Aral Sea (lower panel) in comparison with the mass change observed by GRACE (upper panel; left axis) and the total Aral Sea surface area (upper panel; right axis).

Fig. 9: Quantitative comparison between the total Aral Sea surface area and GRACE mass change (data taken from Fig. 7).

Figure 1

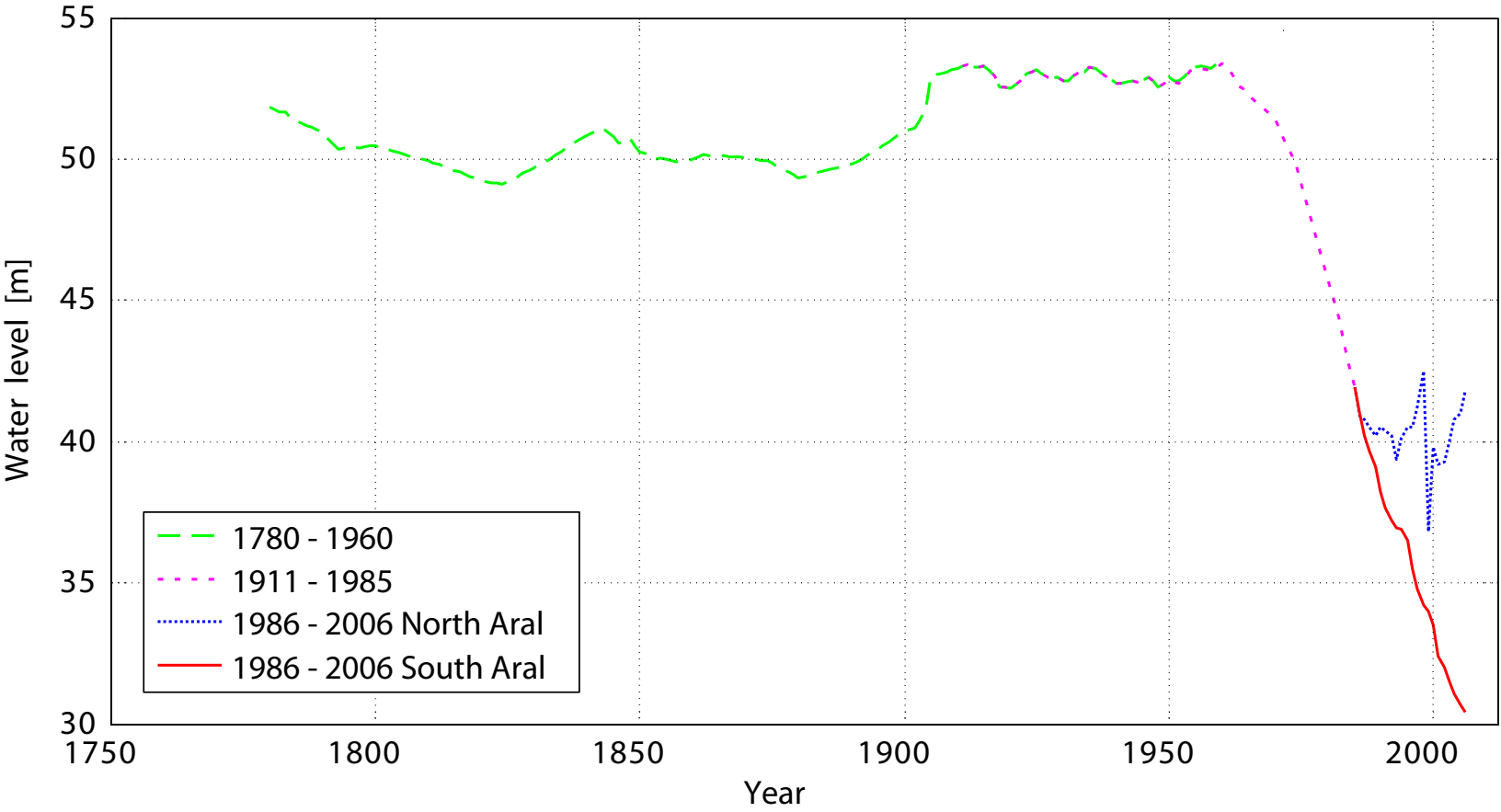
55
50
45
40
35
30
Water level [m]
1750
1800
1850
1900
1950
2000
Year
1780 - 1960
1911 - 1985
1986 - 2006 North Aral
1986 - 2006 South Aral

Figure 2

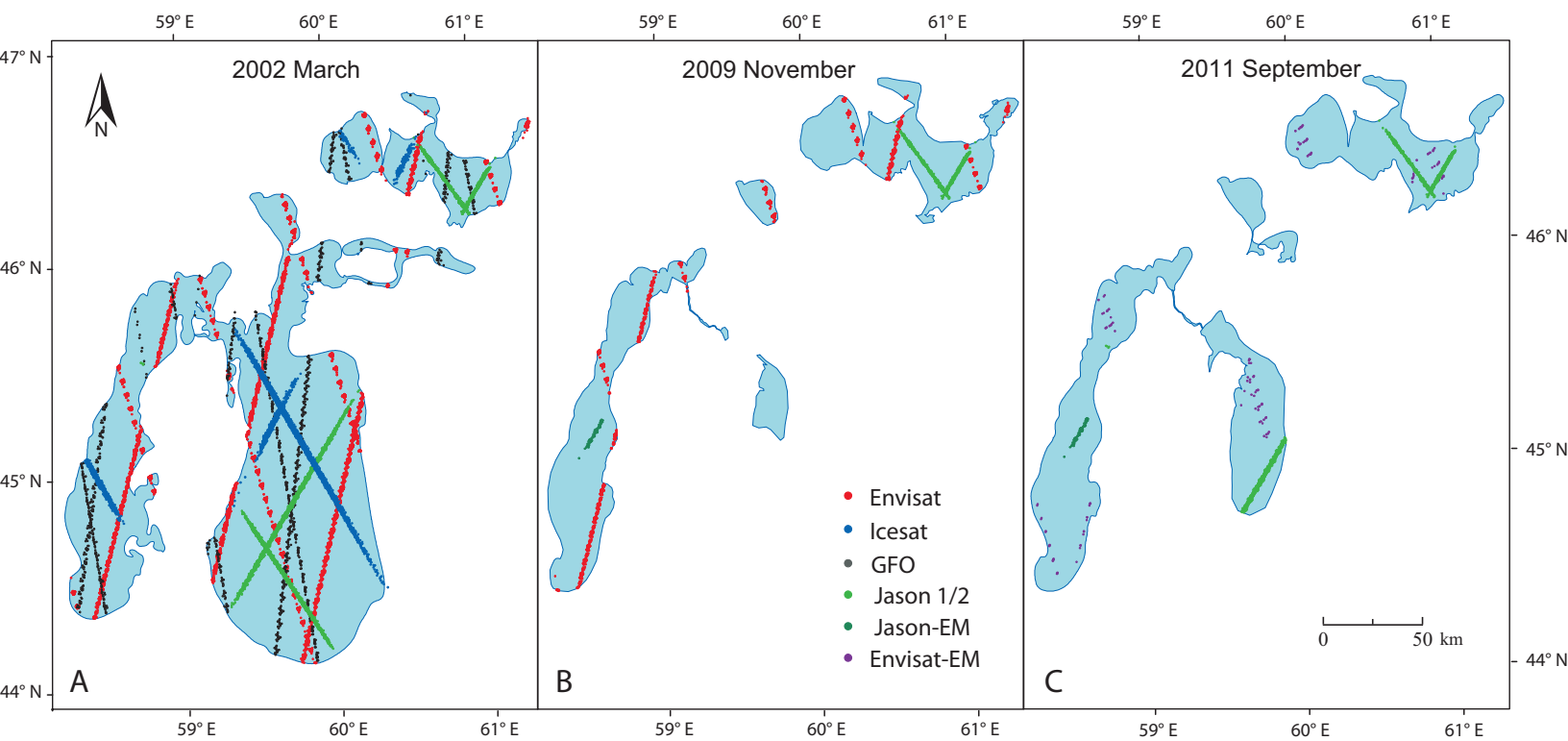
59° E
60° E
61° E
47° N
46° N
45° N
44° N
2002 March
N
A
2009 November
B
2011 September
C
Envisat
Icesat
GFO
Jason 1/2
Jason-EM
Envisat-EM
0
50 km

Figure 3

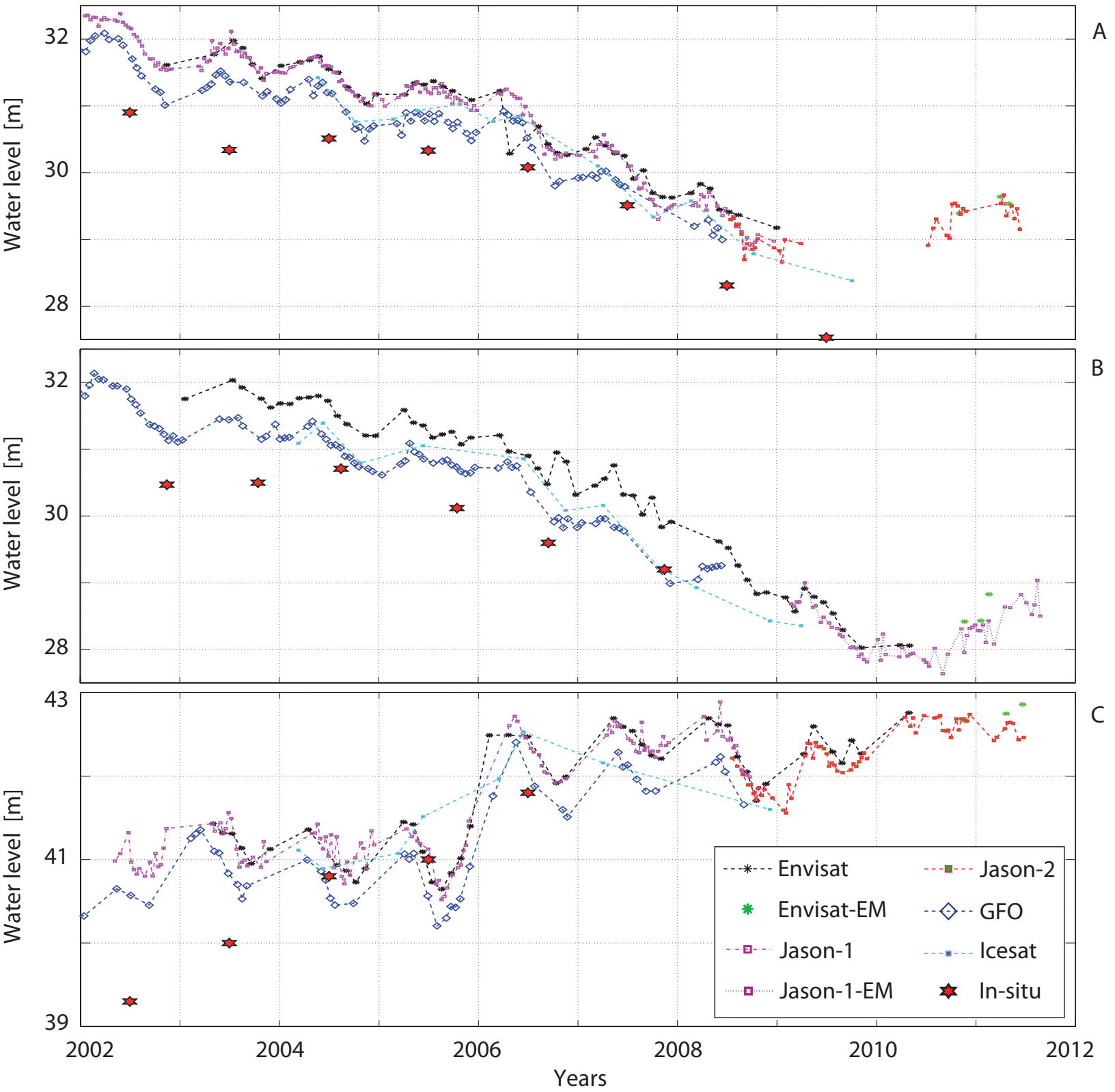
A
B
C
Water level [m]
32
30
28
43
41
39
2002
2004
2006
2008
2010
2012
Years
Envisat
Envisat-EM
Jason-1
Jason-1-EM
Jason-2
GFO
Icesat
In-situ

Figure 4

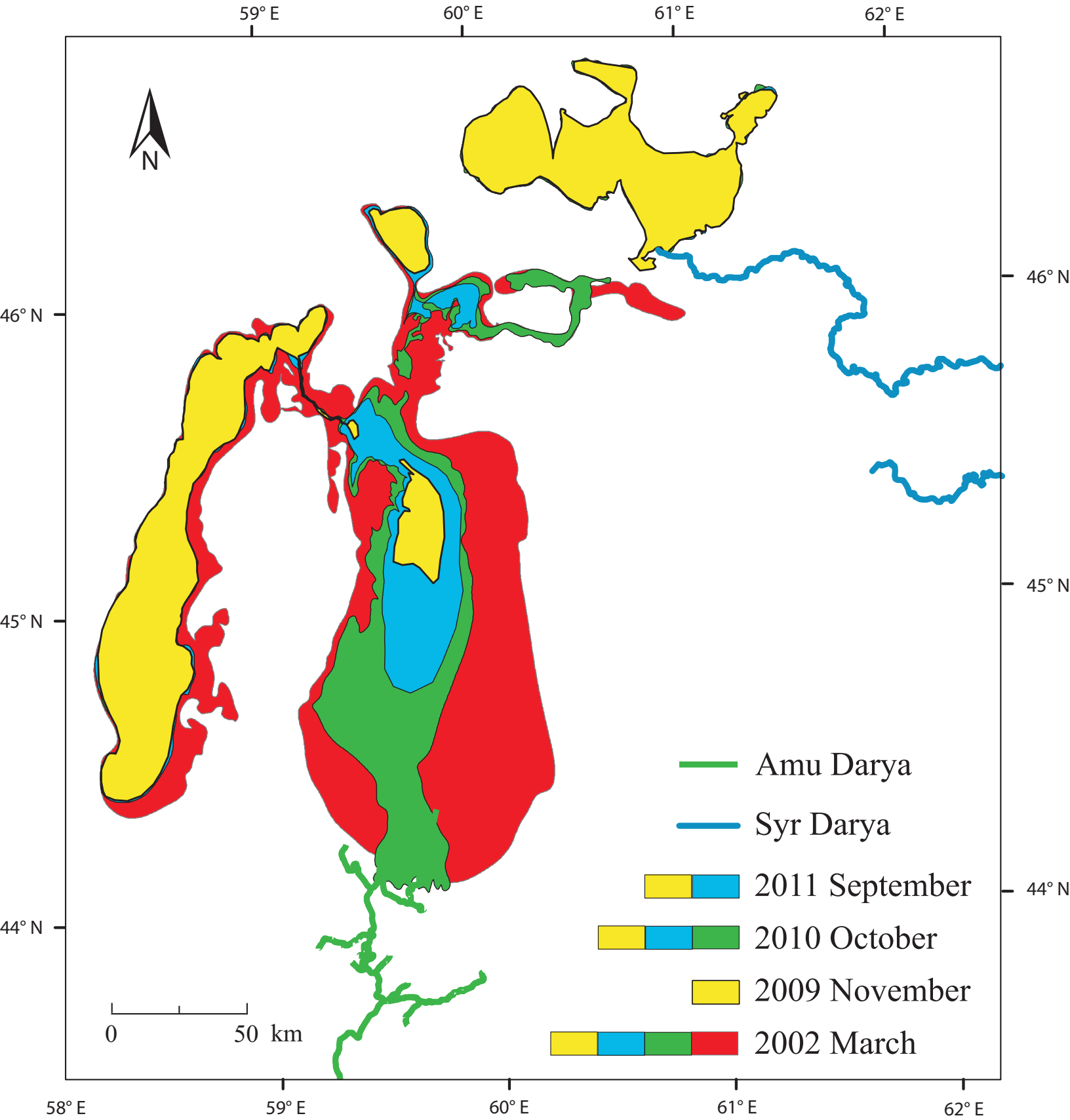
59° E
60° E
61° E
62° E
N
46° N
45° N
44° N
0
50 km
Amu Darya
Syr Darya
2011 September
2010 October
2009 November
2002 March
58° E
59° E
60° E
61° E
62° E

Figure 5

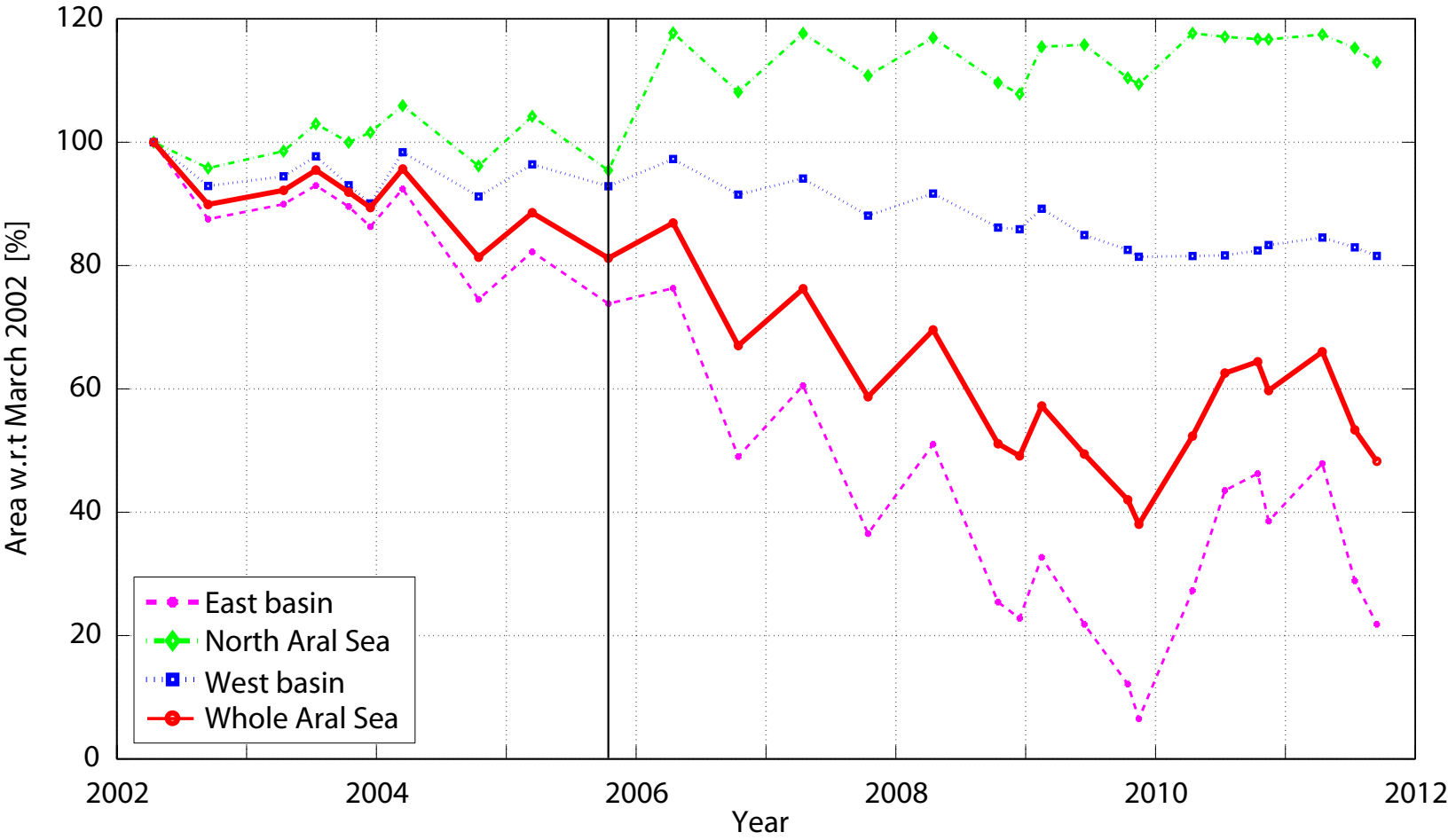
120
100
80
60
40
20
0
2002
2004
2006
2008
2010
2012
Year
Area w.r.t March 2002 [%]
East basin
North Aral Sea
West basin
Whole Aral Sea

Figure 6

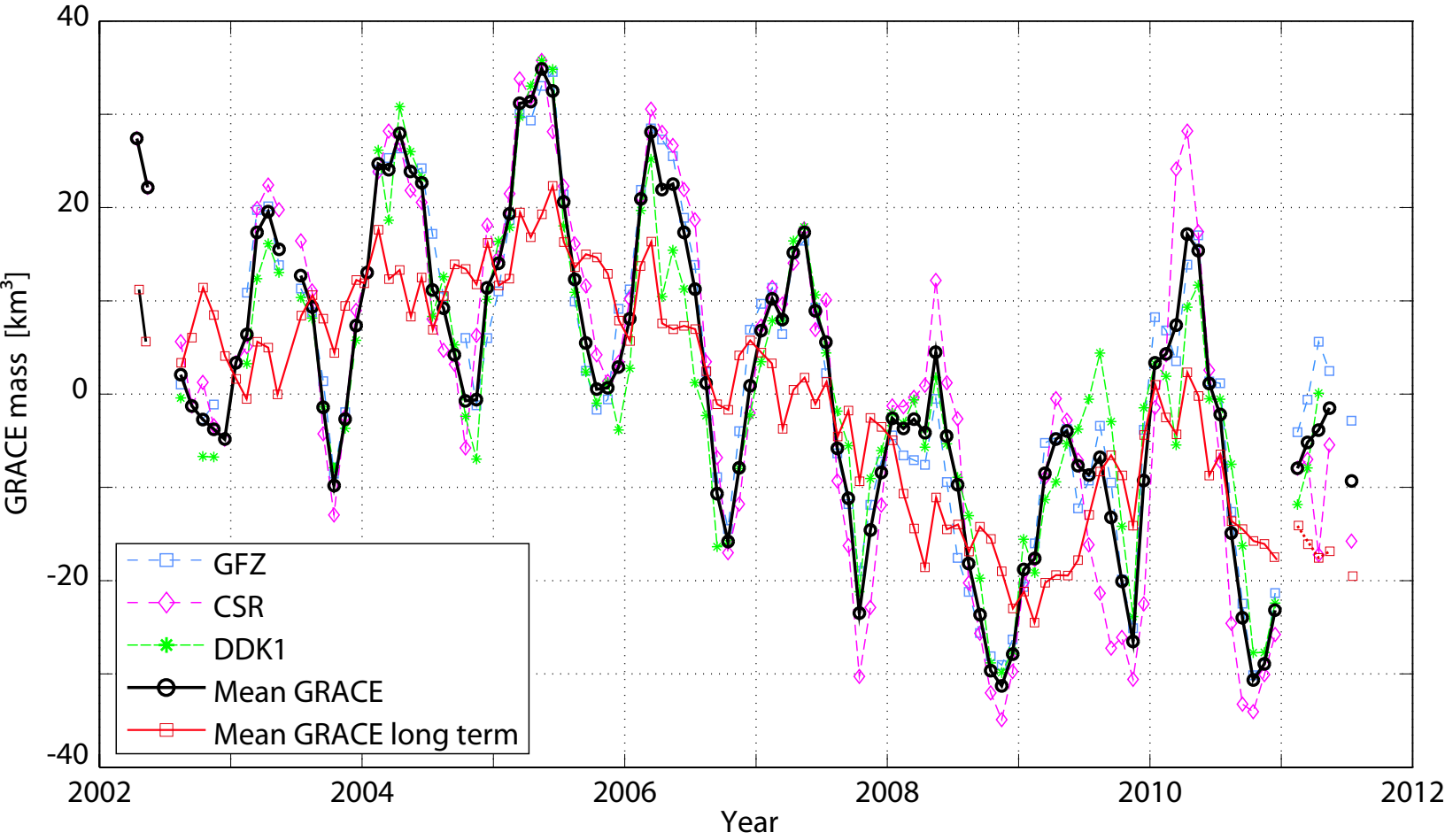
40
20
0
-20
-40
GRACE mass [km³]
2002
2004
2006
2008
2010
2012
Year
GFZ
CSR
DDK1
Mean GRACE
Mean GRACE long term

Figure7

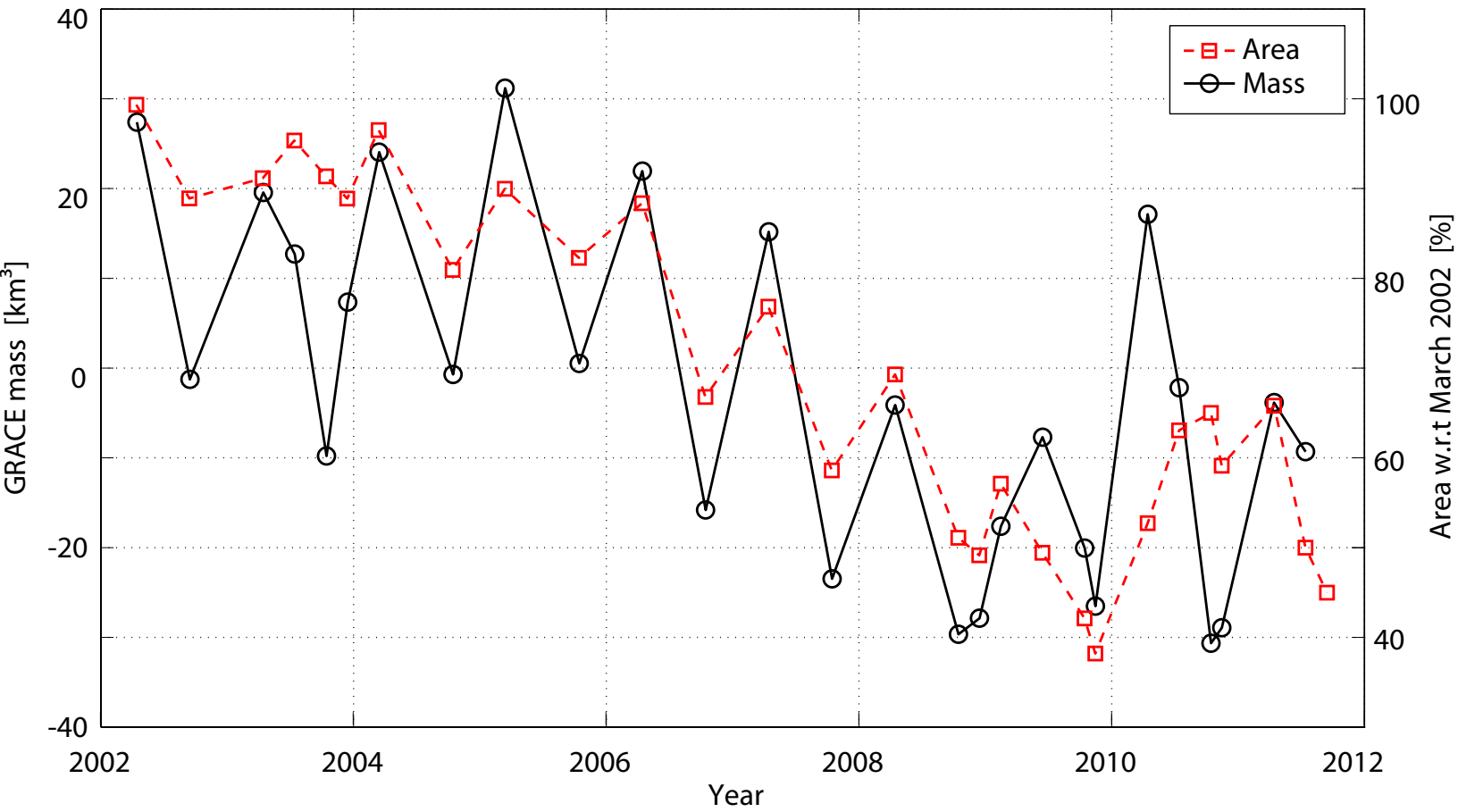
Area
Mass
GRACE mass [km³]
Area w.r.t March 2002 [%]
Year
40
20
0
-20
-40
100
80
60
40
2002
2004
2006
2008
2010
2012

Figure 8

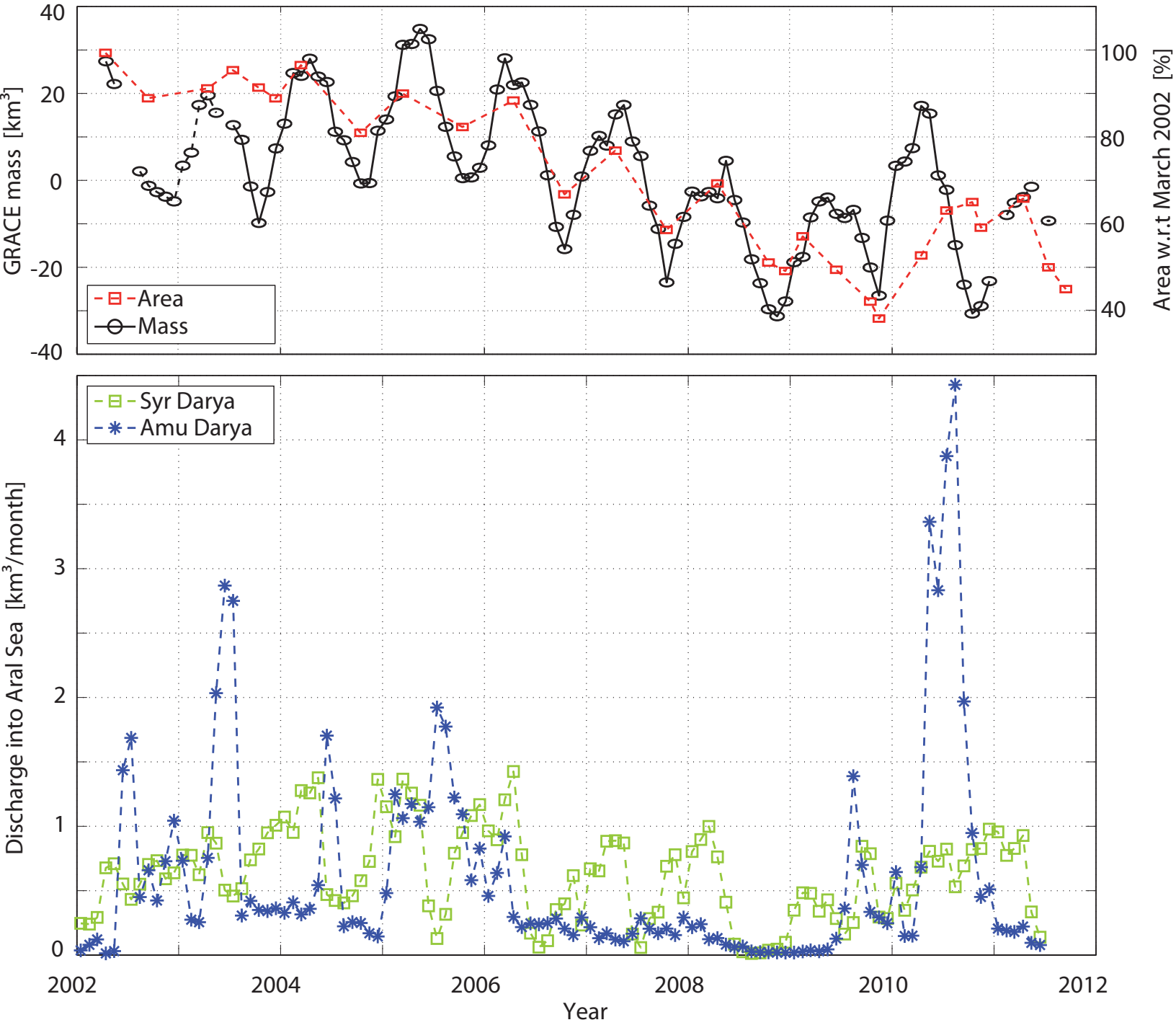
GRACE mass [km³]
Area w.r.t March 2002 [%]
Area
Mass
Syr Darya
Amu Darya
Discharge into Aral Sea [km³/month]
Year
2002
2004
2006
2008
2010
2012

Figure 9

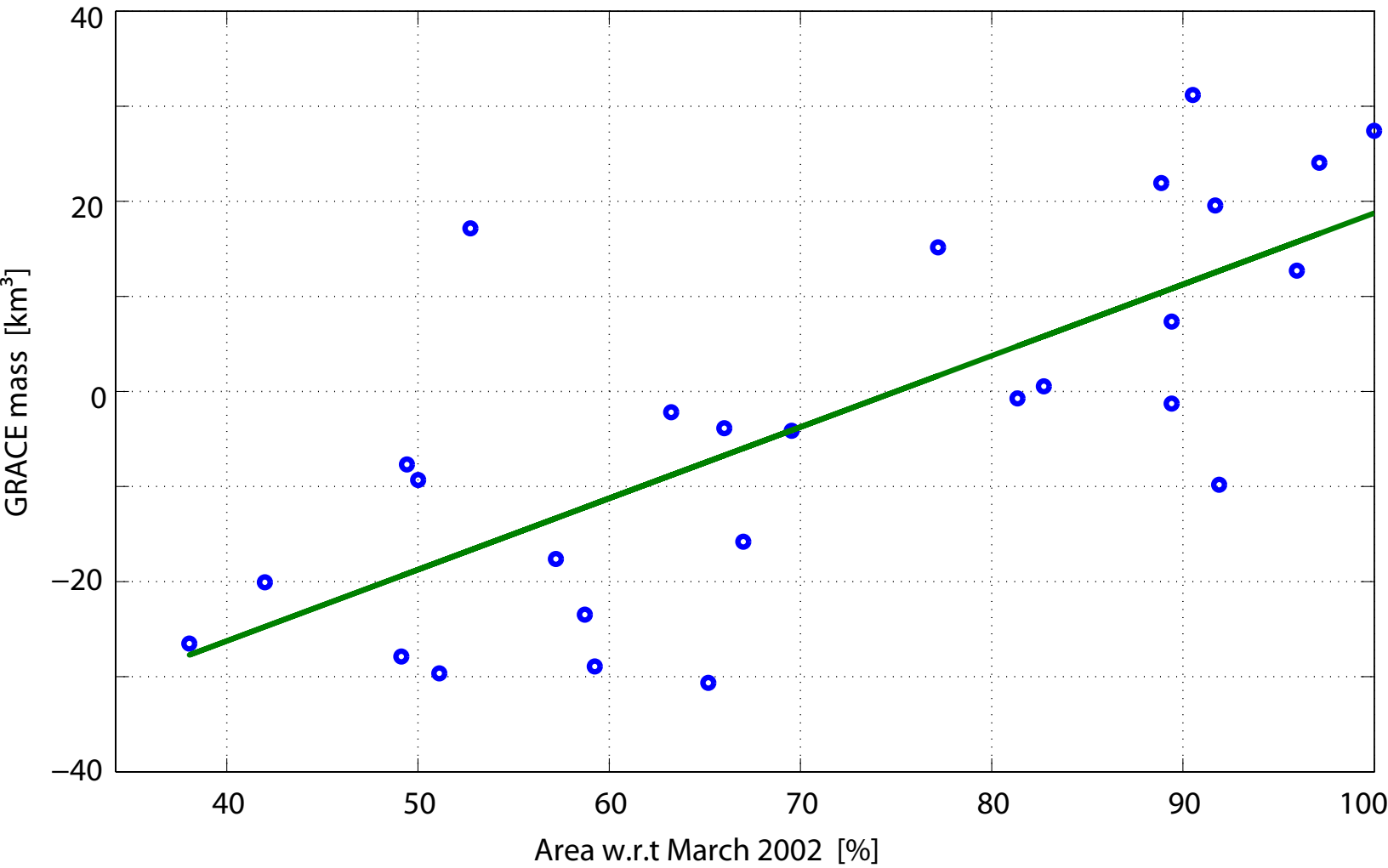
40
20
0
−20
−40
GRACE mass [km³]
40
50
60
70
80
90
100
Area w.r.t March 2002 [%]